Research on Chemical Intermediates (2022) 48:2593–2606
https://doi.org/10.1007/s11164-022-04727-4

Solvent-free catalytic oxidation of toluene over heterogeneous $CeMnO_x$ composite oxides

Gui Chen[1,3] · Kuiyi You[1,2] · Fangfang Zhao[1] · Zhenpan Chen[1] · Hean Luo[1,2]

Received: 10 January 2022 / Accepted: 18 April 2022 / Published online: 12 May 2022

Abstract

An inexpensive and controllable $CeMnO_x$ composite oxides catalyst for the liquid-phase catalytic oxidation of toluene was conveniently prepared by ultrasound-assisted co-precipitation method. The physical–chemical properties of $CeMnO_x$ composite oxides catalyst have been systematically characterized. MnO_x as catalytic active species was highly dispersed in the cubic fluorite structure CeO_2. The cooperation of CeO_2 and MnO_x evidently improved the catalytic performance. $CeMnO_x$ composite oxides with a Ce/Mn molar ratio of 2:1 was showed the good catalytic performance. 7.0% of toluene conversion and 95.6% of overall selectivity to benzylalcohol, benzaldehyde and benzoic acid was acquired under optimal reaction conditions. The present catalyst has the advantages of low cost, good catalytic performance and stability. This work provides a simple, benign and controllable approach for the selective oxidation of toluene to valuable oxidation products.

Graphical abstract

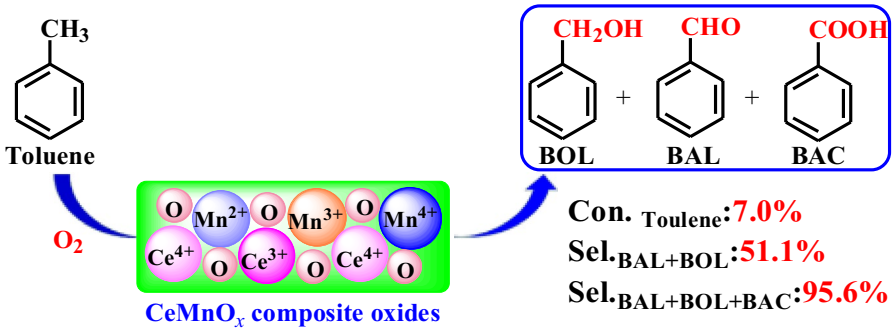

Keywords $CeMnO_x$ composite oxides Liquid-phase catalytic oxidation · Benzylalcohol · Benzaldehyde · Benzoic acid

Extended author information available on the last page of the article

Introduction

Selective oxidation of aromatic hydrocarbons to oxygen-containing chemical products or chemical intermediates like alcohols, aldehydes, acids and other carbonyl compounds is very important process [1, 2]. Usually, these mentioned products are prepared by catalytic aerobic oxidation reaction of alkyl aromatics [3, 4]. As one of the most common alkyl aromatics, the benzene ring side chain C–H bonds of toluene could be selectively catalytic oxidized into three oxygenated organic products: benzaldehyde (BAL), benzyl alcohol (BOL) and benzoic acid (BAC). There is great economic and industrial importance [5–7]. Among them, BAL is an intermediate for the synthesis of amphotericin, ephedrine and chloramphenicol, also is used for preparing aniline dyes, perfume and flavoring compounds [8]. BOL has significant application in the manufacture of drug synthesis, flavor fixing agent, textile printing, artificial fiber desiccant [9]. BAC is used as a chemical intermediate, raw material of sodium benzoate preservative and diverting agent in crude-oil recovery applications [10].

Traditionally, BAL and BOL are mainly produced by chlorination of the -CH_3 group of toluene and hydrolysis. Halogen compounds are used in the process, which is harmful to the environment and limits its widely application [11]. In addition, it also has the disadvantages of equipment corrosion and toxic waste generation [12]. BAC is mainly produced by directly oxidation of toluene with cobalt acetate catalyst, 20–30% toluene conversion and 90% selectivity to BAC were obtained in industry. However, cobalt salt as a homogeneous catalyst is difficult to separate. Even more, cobalt oxalate precipitate is easy to precipitate in the oxidation reaction, leading to serious scale formation in the pipeline [13].

Therefore, it has been widely researched on the selective aerobic oxidation of toluene in recent years, including vapor and liquid-phase oxidation, selective photo-oxidation and electrochemical oxidation, etc. [14–17]. In the above-mentioned processes, the vapor-phase oxidation (reaction temperature 350–550 °C) is easy to deep oxidation with low atomic economy [18, 19], and photo/electrocatalytic reactions also are difficult to achieve in industry [20]. Heterogeneous catalytic oxidation of toluene in liquid-phase system is relatively mild conditions, easy to operate and high selectivity, which is an important technology to transform toluene into industrial important oxygen-containing derivatives [21].

In liquid phase heterogeneous oxidation processes of alkyl aromatics, noble metal oxide catalysts supported by Au, Pt or Pd are commonly used, because of their high activity and selectivity [11, 22, 23]. However, due to the limited and expensive precious metals, transition metal oxide catalysts are also considered as cheap substitutes for precious metals and are highly valued by researchers [24, 25]. To improve the performance of transition metal oxide catalysts, it is necessary to optimize the dispersion of active metal species and/or to achieve synergies between different species by forming mixed oxides [26, 27]. Because of the high activity and functional adaptability versatility of Ce-Mn oxides system, it has the potential industrial applications, such as the catalytic wet oxidation of waste waters tetracycline [28], the decomposition of NO_x [29] and the combustion of

volatile organic compounds [30]. Ce-Mn oxides has the good catalytic activity due to the synergistic interactions between manganese oxides and cerium oxides [31]. Herein, MnO_x as active species in the Ce-Mn oxide was highly dispersed, and CeO_2 as an accelerator can increase the oxygen mobility due to its unique oxygen storage capacity [32, 33].

Based on the above reasons and some previous works about liquid phase aerobic catalytic oxidation reactions under solvent-free conditions [34–38], we will report the $CeMnO_x$ composite oxides catalyst for the catalytic oxidation of toluene using dioxygen as the oxidant. The reaction conditions such as oxygen pressure, reaction temperature, reaction time and catalyst amount were optimized. The chemical and physical properties of $CeMnO_x$ composite oxides were studied by various characterization techniques. It is shown that this method is a promising process for the synthesis of BOL, BAL and BAC in the industrial applications.

Experimental

Reagents and instrument

Cerium(III) nitrate hexahydrate ($Ce(NO_3)_3 \bullet 6H_2O$, AR, 99.0%) and toluene (C_7H_8, AR, 99.5%) were gained from Sinopharm Group Co., Ltd. Manganese(II) nitrate ($Mn(NO_3)_2$) 50% aqueous solution was obtained from Shanghai Mclean Co., ltd, China. The quantitative and qualitative analysis of products was performed on Gas chromatography (GC Agilent 7890B) and Gas chromatography-mass spectrometry, respectively.

Catalyst preparation

$CeMnO_x$ composite oxides catalyst was prepared by the ultrasound-assisted co-precipitation method [39]. Typically, 4.4 g $Mn(NO_3)_2$ and 1.8 g $Ce(NO_3)_3 \cdot 6H_2O$ were dissolved into 20 mL of deionized water, and then 0.45 mol/L potassium carbonate solution was slowly dropped under stirring. Subsequently, the precipitate was treated by ultrasound for 0.5 h, and the pH was adjusted at 9.0 with ammonia. The mixture was stirred at room temperature for 4.0 h, and aged for 2.0 h. Lastly, the sediment was washed to neutrality, dried overnight and calcined at 400 °C for 2.0 h to obtain the $CeMnO_x$ oxides catalyst.

Catalyst characterizations

The textural properties were recorded by N_2 physisorption on a TriStar II 3020 at 77 K. XRD data of samples were performed on a Rigaku D/Max-2550/VB^+ 18 kW diffractometer with monochromatic Cu Kα as radiation ($\lambda = 1.5418$ A) source at 40 kV and 250 mA. The chemical states of elements were analysed by an ESCALAB 250Xi analyser. H_2-TPR spectra were collected on an Auto Chem II 2920. The SEM

and HRTEM images were recorded on a JSM-6610LV spectrometer and a JEM-2100, respectively.

Catalytic reaction process

The reaction was implemented in 50 mL autoclave. Typically, 0.1 g $CeMnO_x$ oxides and 21.0 g toluene were weighed into the reactor and heated to pre-set temperature at constant stirring of 800 rpm. Then dioxygen was pumped into the autoclave reactor system, and the reaction was kept at 0.6 MPa pressure with 180 °C for 4.0 h. After the reaction finished, the liquid phase products were analyzed by GC.

Results and discussion

Catalytic activity of diverse catalysts

Table 1 investigated diverse catalysts in the reaction. In the absence of catalysts, three oxidation products could be obtained with toluene conversions of only 2.5% (entry 1). Compared with other single metal oxide catalysts, MnO_x exhibited better catalytic performance in the oxidation reaction (entries 2–5). In order to further enhance the catalytic performance of MnO_x, we attempted to add other metal

Table 1 Catalytic activity comparison in the oxidation of toluene[a]

Entry	Catalyst	Conversion (%)	Selectivity (%)				
			BAL	BOL	BAC	Total[b]	Others[c]
1	None	2.5	44.1	33.7	20.1	97.9	2.1
2	CuO	2.2	59.4	16.4	22.6	98.4	1.6
3	Co_3O_4	2.4	47.0	33.1	19.9	100	0.0
4	CeO_2	0.4	90.7	4.7	4.6	100	0.0
5	MnO_x	5.6	29.1	15.6	49.9	94.6	5.4
6	$CeMnO_x$	7.0	26.3	24.8	44.5	95.6	4.4
7	$LaMnO_x$	6.0	29.9	21.3	39.8	91.0	9.0
8	$CrMnO_x$	6.5	30.4	22.1	41.2	93.7	6.3
9	$CeO_2 + MnO_x$[d]	4.9	30.6	19.2	45.9	95.7	4.3
10	$CeMnO_x$[e]	19.2	10.6	10.8	66.9	88.3	11.7
11	$CeMnO_x$[f]	41.5	1.6	0.6	75.1	77.3	22.7

[a]Reaction conditions: O_2: 0.6 MPa, temperature: 180 °C, time: 4.0 h, toluene: 21.0 g, catalyst: 0.1 g

[b]Total delineated the total selectivity to BOL + BAL + BAC

[c]Others were benzyl benzoate, benzyl formate, 2-methylbiphenyl, 4-methylbiphenyl and 1,4-benzoquinone

[d]CeO_2 and MnO_x were physically mixed

[e]O_2: 1.5 MPa, temperature: 180 °C, time:8.0 h, toluene: 21.0 g, catalyst: 0.1 g

[f]Oxidizer TBHP: 10.8 g, toluene: 5.5 g, temperature: 90 °C, time:12 h

element to form Mn-base oxides (entries 6–8). Obviously, compared with MnO_x, CeO_2 or physical blending $CeO_2 + MnO_x$ (entry 9), the addition of CeO_2 into the in-situ synthesis of MnO_x improved the catalytic performance in the oxidation reaction. Moreover, we also measured the specific surface area of all Mn related oxides. The results demonstrated that the specific surface areas of MnO_x, $CeMnO_x$, $LaMnO_x$ and $CrMnO_x$ were 32.1, 92.4, 22.5 and 17.7 m^2/g, respectively. It showed that $CeMnO_x$ had relatively high specific surface area. In addition, a high toluene conversion could be obtained by changing the reaction conditions or oxidizer (*tert*-butyl hydroperoxide, TBHP) (entries 10–11). Obviously, the selectivity to BOL and BAL decreased, and the by-products increased significantly. Therefore, among these oxides catalysts, the acceptable 7.0% of toluene conversion with 95.6% total selectivity to BOL, BAL and BAC were gained over $CeMnO_x$ composite oxides catalyst.

Effects of Ce/Mn molar ratios of catalysts on the reaction

Table 2 inventoried the results of oxidation of toluene by catalysts with different Ce/Mn molar ratios. With the increase of Mn in the catalyst, the conversion of toluene showed an incremental trend. An appropriate result with 7.0% of toluene conversion and 95.6% total selectivity to three products was obtained with Ce/Mn molar ratio of 2:1. From the surface area of $CeMnO_x$ composite oxides with different molar ratio of cerium and manganese, $CeMnO_x$ composite oxides catalyst at 2:1 of Ce/Mn has relatively high surface area. Maybe appropriate molar ratio of cerium and manganese is conducive to the dispersion of active species (MnO_x).

Effects of various factors on toluene oxidation

Figure 1 optimized the parameters for the oxidation reaction. As Fig. 1A, B shown, the toluene conversion and BAC selectivity were increased while BAL, BOL selectivity decreased as the increase of reaction pressure and time. This was a major cause

Table 2 Effects of the different Ce/Mn molar ratios of catalysts on the reaction[a]

Ce/Mn	Conversion (%)	Selectivity (%)				
		BAL	BOL	BAC	Total	Others
5:1	3.7	40.5	23.7	32.0	96.2	3.8
3:1	5.2	33.3	22.0	40.7	96.0	4.0
2:1	7.0	26.3	24.8	44.5	95.6	4.4
1:1	7.4	27.9	17.7	46.1	91.7	8.3
1:3[b]	7.1	25.6	24.5	44.3	94.4	5.6
1:5[c]	6.9	26.4	24.0	43.4	93.8	6.2

[a]Reaction conditions: O_2: 0.6 MPa, temperature: 180 °C, time: 4.0 h, toluene: 21.0 g, catalyst: 0.1 g. unless otherwise indicated

[b]3.0 h

[c]0.8 MPa, 2.0 h

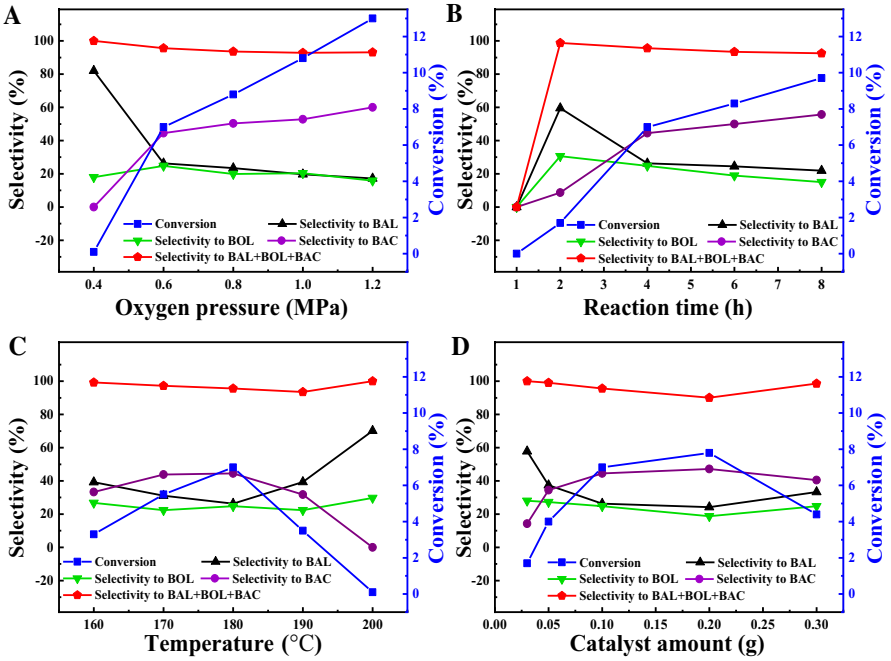

Fig. 1 Effects of different factors on the reaction. Reaction conditions: **A** temperature: 180 °C, catalyst: 0.1 g, time: 4.0 h, toluene: 21.0 g; **B** O_2: 0.6 MPa, temperature: 180 °C, toluene: 21.0 g, catalyst: 0.1 g; **C** O_2: 0.6 MPa, time: 4.0 h, toluene: 21.0 g, catalyst: 0.1 g; **D** O_2: 0.6 MPa, temperature: 180 °C, time: 4.0 h, toluene: 21.0 g

that BAL and BOL could further oxidize to BAC and by-products in this process. In a certain range, the conversion of toluene gradually increased with elevated reaction temperature and catalyst dosage, and then it showed an opposite trend (Fig. 1C, D). For the catalyst, excessive catalyst was apt to agglomerate, so that the catalytic activity could not be fully demonstrated [37]. For reaction temperature, with the increase of temperature, the vapor pressure of toluene in the reactor was increased in the gas phase, and the injected oxygen was actually decreased [38]. From the results of single-factor experiment, the appropriate reaction conditions were acquired: reaction oxygen pressure is 0.6 MPa, reaction time is 4.0 h, reaction temperature is 180 °C and catalyst dosage is 0.1 g. 7.0% of toluene conversion and 95.6% three products selectivity were achieved.

Recycling of $CeMnO_x$ composite oxides catalyst

Figure 2 showed the reusability of catalyst in the reaction. Obviously, the conversion of toluene and the total selectivity to three products were not changed significantly after five runs. The results demonstrated that the catalyst possessed good stability and satisfactory reusability.

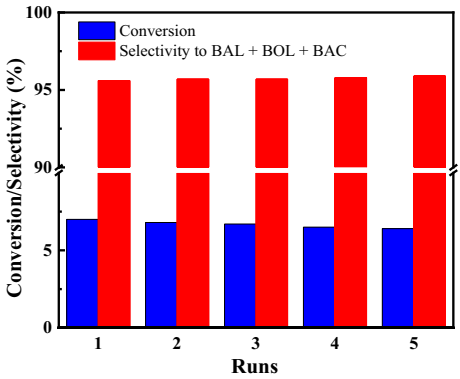

Fig. 2 Reusability of $CeMnO_x$ composite oxides. O_2: 0.6 MPa, temperature: 180 °C, time: 4.0 h, toluene: 21.0 g, catalyst: 0.1 g

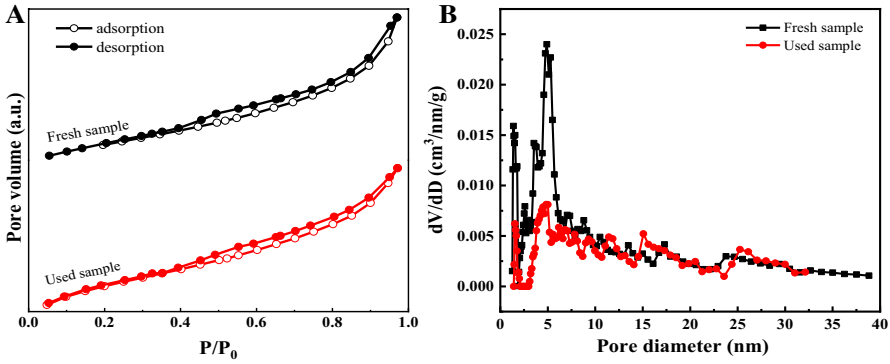

Fig. 3 N_2 adsorption–desorption isotherms **A** and pore diameter curves **B** of two samples

Table 3 Textural properties of two samples

Samples	Surface area (m^2/g)	Pore volume (cm^3/g)	Pore diameter (nm)
Fresh $CeMnO_x$	92.4	0.16	7.0
Used $CeMnO_x$	84.7	0.11	8.7

Catalyst characterization

Nitrogen adsorption–desorption isotherms of $CeMnO_x$ composite oxides are shown in Fig. 3A. Two samples are type II isotherms with type H3 hysteresis loop [40]. This indicates that the samples belong to mesoporous structure materials [41, 42]. In Fig. 3B, it can be seen that the pore diameter distribution of two samples is irregular, which is caused by the difference of the crystal phases with diverse granularity in the micro-sizes and meso-sizes [38]. In addition, as shown in Table 3, the textural properties parameters of $CeMnO_x$ composite oxides catalyst are only mildly change after five runs.

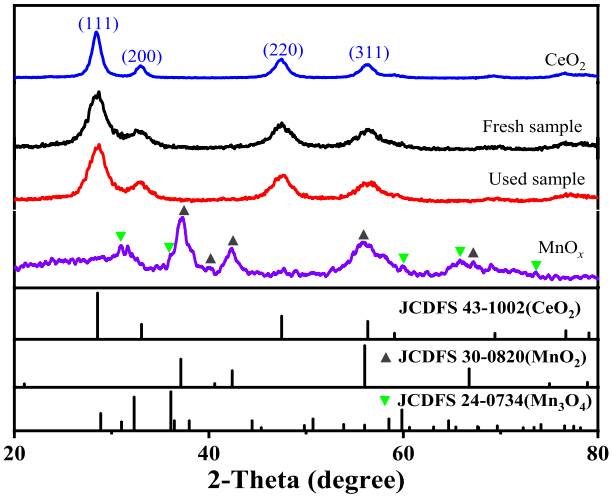

Fig. 4 XRD patterns of samples

The XRD spectra of samples are shown in Fig. 4. Obviously, CeO_2 has a cubic fluorite structure (JCPDS 43–1002) [43]. MnO_x has a certain crystal structure (JCPDS 30–0820 and JCPDS 24–0734). With the increases of manganese content of two samples, the characteristic peaks of MnO_x in the $CeMnO_x$ composite oxides are gradually strong, and its crystallinity is decreased. However, only diffraction peaks of CeO_2 are detected in the fresh and used samples, demonstrating manganese species are uniformly highly dispersed in cubic fluorite structure CeO_2 [44]. This result is consistent with the report by Machida et al. [45]. Among Mn^{4+}, Mn^{3+} and Mn^{2+}, the largest ion radius is Mn^{2+} (0.083 nm), which is smaller than Ce^{3+} (0.087 nm), instructing that a certain amount of Mn species are doped into CeO_2 lattice to decrease crystallinity of the catalyst [29, 46, 47].

Figure 5 shows the XPS spectra of fresh and used samples. In Fig. 5A, it displays the characteristic peaks of C 1 s (284.8 eV), O 1 s (529.0 eV), Mn $2p_{3/2}$ (641.2 eV) and Ce 3d (897.4 eV), respectively. Figure 5B shows the Ce 3d XPS spectra. Six peaks labeled as 915.7, 906.5, 900.2, 897.5, 881.6 and 888.1 eV are assigned to Ce^{4+} species, and the peaks centered at 901.3 and 882.8 eV are assigned to Ce^{3+} species [30]. The Ce^{3+} species can form oxygen vacancy and unsaturated chemical bonds in the catalysts [48]. Figure 5C displays the Mn $2p_{3/2}$ XPS spectra. The peak at 642.9 eV corresponds to superficial Mn^{4+}, while the other peaks at 641.6 and 640.6 eV correspond to the superficial Mn^{3+} and Mn^{2+}, respectively [49, 50]. Figure 5D displays the O 1 s XPS spectra. The peak at 533.9 eV is assigned to physical adsorbed H_2O, and the second peak in the middle (531.1 eV) is attributed to chemisorption oxygen, the peak at the lower binding energy (529.0 eV) is attributed to lattice oxygen [51, 52]. It can be seen that the valence states of the three elements of the catalysts are unchanged before and after the reaction, which is one of the reasons for its good stability.

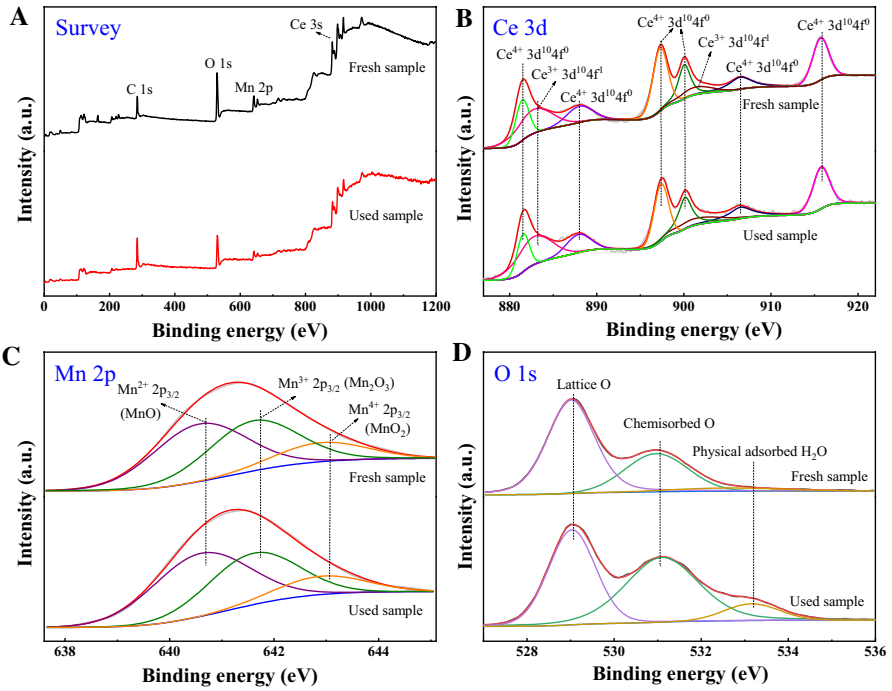

Fig. 5 XPS spectra of samples

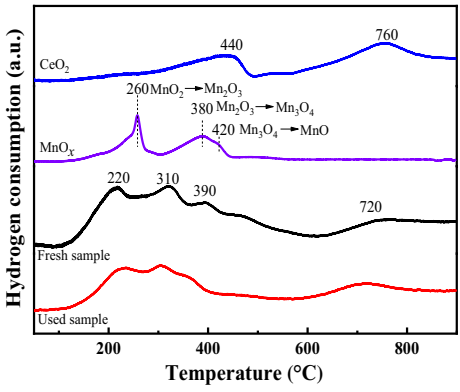

Fig. 6 H_2-TPR curves of samples

Figure 6 shows the H_2-TPR spectra of fresh and used samples. Clearly, CeO_2 exhibits two visible peaks at 440 and 760 °C, respectively. The low temperature reduction peak is due to reaction of hydrogen by superficial Ce^{4+}, and the second peak is connected with the obvious reduction of Ce^{4+} to Ce^{3+} in bulk CeO_2 [53, 54]. MnO_x exhibits three reduction peaks located at 260, 380 and 420 °C due to the reduction of MnO_2 to Mn_2O_3, Mn_2O_3 to Mn_3O_4, and Mn_3O_4 to MnO, respectively [33, 55]. Compared with the bulk CeO_2 and MnO_x, fresh and used samples exhibit

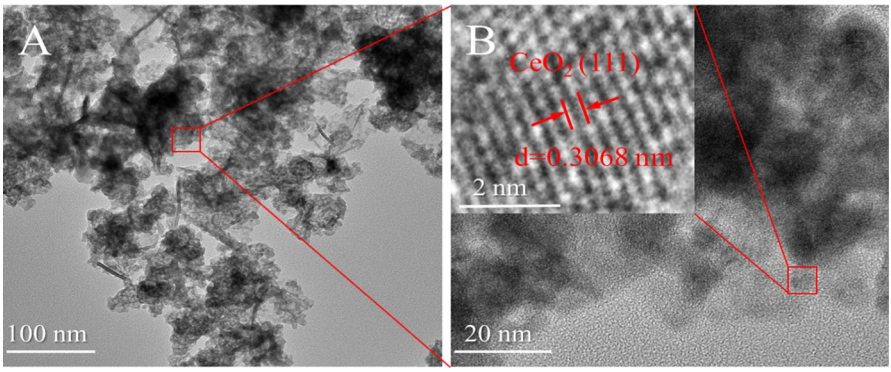

Fig. 7 TEM images of the fresh sample

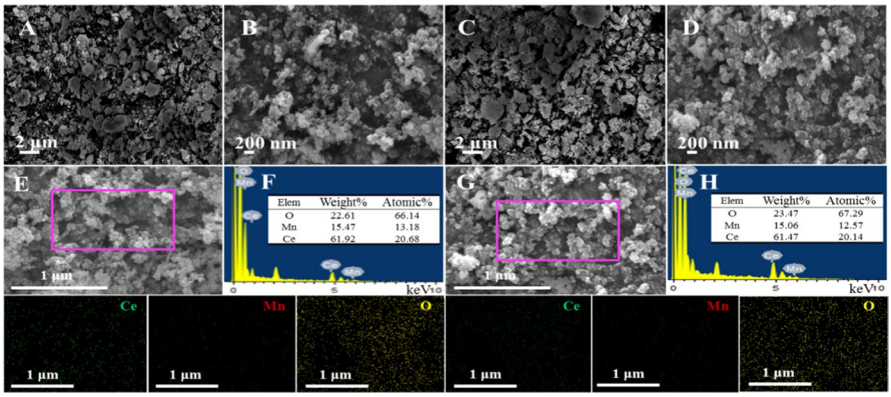

Fig. 8 SEM, EDS and Mapping images of (**A**, **B**, **E**, **F**) fresh and (**C**, **D**, **G**, **H**) used samples

three reduction peaks at ~ 220, ~ 310 and ~ 390 °C, attributing to the reduction of MnO_x species in the $CeMnO_x$ composite oxides [49]. It was noticed that fresh and used samples display the lower reduction temperature, meaning the improvement of lattice oxygen migration ability [56]. Combined with Table 1, XRD and XPS analysis, it can be seen that the catalytic performance of $CeMnO_x$ composite oxides is improved, MnO_x is the main oxidative active species, and Ce^{4+}/Ce^{3+} pairs provides the lattice defects and oxygen vacancies to increase the oxygen mobility.

TEM images of fresh catalyst shown in Fig. 7. It is clearly observed the lattice spacing of the catalyst. Moreover, the measured lattice spacing of $CeMnO_x$ composite oxides is 0.31 nm, which is basically consistent with the plane of CeO_2 (111) [30, 57]. However, in the HRTEM images of the samples, no lattice fringes of MnO_x were recognized, combined with XRD analysis, it indicated that MnO_x are highly dispersed in CeO_2.

The fresh and used samples are flake-like, and the basically morphology does not change in Fig. 8A–D. EDS and mapping images indicate that Ce, Mn and O

elements are presence and uniform distribution in two samples (Fig. 8E–F). The catalyst has excellent catalytic activity in catalytic oxidation of toluene reaction because of the homogeneous distribution of MnO_x [58]. Furthermore, compared with the fresh catalyst, the weight or atomic ratio of Ce and Mn does not change much on the used catalyst, indicating that it is rarely leached during the reaction process.

Possible simple pathway for the formation of products during $CeMnO_x$ composite oxides in the reaction

In accordance with the above results and previous reports [59, 60], a possible pathway for the formation of products in the catalytic oxidation of toluene was proposed, as shown in Fig. 9. The toluene is adsorbed over $CeMnO_x$ composite oxides. Due to the synergy interaction of manganese ions and cerium ions with different valence states in the catalyst, the adsorbed toluene was activated to benzyl radical ($C_7H_7^{\bullet}$) by extracting hydrogen over active MnO_x species [1, 61]. The $C_7H_7^{\bullet}$ reacts with O_2 to generate benzyl methyl peroxide radicals ($C_7H_7OO^{\bullet}$), which is further transformed to benzyl hydroperoxide (C_7H_7OOH) intermediate [60, 61]. Finally, the resulting C_7H_7OOH intermediate is reduced to BOL or decomposed to BAL, and BAL can be further oxidized into BAC.

Conclusions

In conclusion, a simple and viable green method for selective synthesis of BOL, BAL and BAC from oxidation of toluene over $CeMnO_x$ composite oxides without solvent has been developed. It has demonstrated that $CeMnO_x$ composite oxides was an effective simple and inexpensive catalyst for selective oxidation of toluene,

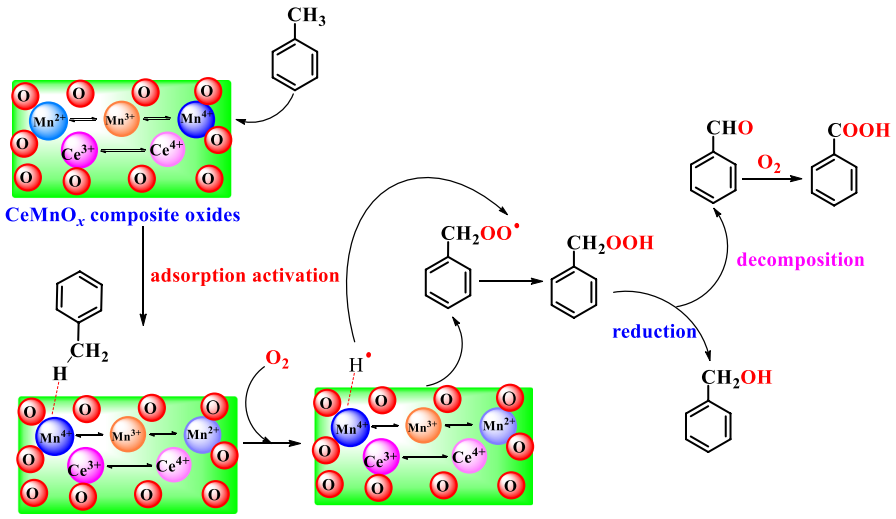

Fig. 9 Schematic reaction pathway for the formation of products over $CeMnO_x$ composite oxides

and 95.6% of total selectivity to three products with 7.0% of toluene conversion was obtained. The active MnO_x homogeneous dispersed in the CeO_2 and the synergistic interaction of Ce and Mn ions during the oxidation reaction were responsible for the good catalytic performance of the catalyst. This method is a promising process for the synthesis of BOL, BAL and BAC in the industrial applications from the toluene with dioxide over $CeMnO_x$ composite oxides catalyst under solvent-free mild conditions.

Acknowledgements The authors are grateful for the financial support of the National Natural Science Foundation of China (21676226), Key Research and Development Program in Hunan Province (2019GK2041), Outstanding Youth Project of Hunan Education Department (20B550), Natural Science Foundation of Hunan Province (2021JJ40531), Hunan Key Laboratory of Environment Friendly Chemical Process Integrated Technology and Collaborative Innovation Center of New Chemical Technologies for Environmental Benignity and Efficient Resource Utilization.

References

1. L. Kesavan, R. Tiruvalam, M.H.A. Rahim, M.I.B. Saiman, D.I. Enache, R.L. Jenkins, N. Dimitratos, J.A. Lopez-Sanchez, S.H. Taylor, D.W. Knight, C.J. Kiely, G.J. Hutchings, Science **331**, 195 (2011)
2. A. Cai, H. He, Q. Zhang, Y. Xu, X. Li, F. Zhang, X. Fan, W. Peng, Y. Li, ACS Appl. Mater. Interfaces **13**, 13087 (2021)
3. Q. Zheng, J. Chen, G. Rao, Russ. J. Org. Chem. **55**, 569 (2019)
4. H. Kargar, M. Fallah Mehrjardi, R. Behjatmanesh Ardakani, K.S. Munawar, M. Ashfaq, M.N. Tahir, Transit. Met. Chem. **46**, 437 (2021)
5. M. Nawab, S. Barot, R. Bandyopadhyay, New J. Chem. **43**, 4406 (2019)
6. Y. Zhuang, Q. Lin, L. Zhang, L. Luo, Y. Yao, W. Lu, W. Chen, Particuology **24**, 216 (2016)
7. H. Göksu, K. Cellat, F. Şen, Nature **10**, 9656 (2020)
8. S. Gopinath, G. Kumar, S. Narayanan, C. Ragupathi, S.S. Kumar, K. Sivakumar, K. Saravanan, S. Ambika, SN Appl. Sci. **1**, 520 (2019)
9. Y. Li, X. Huang, Y. Li, Y. Xu, Y. Wang, E. Zhu, X. Duan, Y. Huang, Sci. Rep. **3**, 1787 (2013)
10. J. Jia, X. Chen, L. Zhai, Y. Niu, Monats. Chem. **151**, 1549 (2020)
11. M. Mo, M. Zheng, J. Tang, Y. Chen, Q. Lu, Y. Xun, Res. Chem. Intermed. **41**, 4067 (2015)
12. J. Lv, Y. Shen, L. Peng, X. Guo, W. Ding, Chem. Commun. **46**, 5909 (2010)
13. J. Miki, Y. Osada, T. Konoshi, Y. Tachibana, T. Shikada, Appl. Catal. A: Gen. **137**, 93 (1996)
14. S. Devika, B. Sundaravel, M. Palanichamy, V. Murugesan, J. Nanosci. Nanotechnol. **14**, 3187 (2014)
15. G. Song, L. Feng, J. Xu, H. Zhu, Res. Chem. Intermed. **44**, 4989 (2018)
16. N. Venkatathri, Indian J. Chem. A **43**, 2325 (2004)
17. Y. Zhu, H. Wang, K. Jin, J. Gong, Chem. A Eur. J. **25**, 6963 (2019)
18. G. Huang, J. Luo, C.C. Deng, Y.A. Guo, S.K. Zhao, H. Zhou, S. Wei, Appl. Catal. A: Gen. **338**, 83 (2008)
19. K.H.C. Chen, P. Liu, T. Chen, J. Chen, Inorganics **6**, 118 (2018)
20. T. Aneeja, M. Neetha, C.M.A. Afsina, G. Anilkumar, Catal. Sci. Technol. **11**, 444 (2021)
21. M. Tan, L. Zhu, H. Liu, Y. Fu, S. Yin, W. Yang, Appl. Catal. A Gen. **614**, 118035 (2021)
22. J.C.F. RodríguezReyes, C.M. Friend, R.J. Madix, Catal. Lett. **148**, 1985 (2018)
23. P. Zhang, Y. Gong, H. Li, Z. Chen, Y. Wang, Nat. Commun. **4**, 1593 (2013)
24. C. Ge, L. Xu, J. Sun, H. Liu, Q. Tong, W. Zou, C. Tang, H. Wan, L. Dong, Y. Chen, Res. Chem. Intermed. **47**, 1239 (2021)
25. C. Guo, Q. Liu, X. Wang, H. Hu, Appl. Catal. A Gen. **282**, 55 (2005)
26. W. Zhong, S.R. Kirk, D. Yin, Y. Li, R. Zou, L. Mao, G. Zou, Chem. Eng. J. **280**, 737 (2015)
27. S.S. Acharyya, S. Ghosh, R. Tiwari, B. Sarkar, R.K. Singha, C. Pendem, T. Sasaki, R. Bal, Green Chem. **5**, 2500 (2014)
28. Y. Sun, T. Zheng, G. Zhang, B. Liu, P. Wang, Environ. Sci. Pollut. Res. **25**, 22818 (2018)
29. G. Picasso, R. Cruz, M.D.R.S. Kou, Mater. Res. Bull. **70**, 621 (2015)

30. H. Cheng, J. Tan, Y. Ren, M. Zhao, J. Liu, H. Wang, J. Liu, Z. Zhao, Ind. Eng. Chem. Res. **58**, 16427 (2019)
31. P. Zhang, H. Lu, Y. Zhou, L. Zhang, Z. Wu, S. Yang, H. Shi, Q. Zhu, Y. Chen, S. Dai, Nat. Commun. **6**, 1 (2015)
32. R. Cano, K. Mackey, G.P. McGlacken, Catal. Sci. Technol. **8**, 1251 (2018)
33. H. Azzi, L. Chérif, S. Siffert, Res. Chem. Intermed. **47**, 1009 (2021)
34. W. Ni, K. You, L. Yi, F. Zhao, Q. Ai, P. Liu, H.A. Luo, Ind. Eng. Chem. Res. **60**, 3907 (2021)
35. S. Liu, K. You, J. Jian, F. Zhao, W. Zhong, D. Yin, P. Liu, Q. Ai, H. Luo, J. Catal. **338**, 239 (2016)
36. J. Jian, D. Kuang, X. Wang, H. Zhou, H. Gao, W. Sun, Z. Yuan, J. Zeng, K. You, H. Luo, Mater. Chem. Phys. **246**, 122814 (2020)
37. P. Liu, K. You, R. Deng, Z. Chen, J. Jian, F. Zhao, P. Liu, Q. Ai, H. Luo, Mol. Catal. **466**, 130 (2019)
38. G. Chen, K. You, X. Gong, F. Zhao, Z. Chen, H. Luo, React. Chem. Eng. **7**, 898 (2022)
39. G. Qi, R.T. Yang, R. Chang, Appl. Catal. B Environ. **51**, 93 (2004)
40. K.S.W. Sing, D.H. Everett, R.A.W. Haul, L. Moscou, R.A. Pierotti, J. Rouquerol, T. Siemieniewska, Pure Appl. Chem. **57**, 603 (1985)
41. S.M. Vickers, R. Gholami, K.J. Smith, M.J. MacLachlan, ACS Appl. Mater. Interfaces **7**, 11460 (2015)
42. M. Li, H. Zhu, J. Cheng, M. Zhao, W. Yan, J. Porous Mat. **24**, 507 (2017)
43. W. Han, L. Wu, Y. Zhu, J. Am. Chem. Soc. **127**, 12814 (2005)
44. J. Zhang, Y. Cao, C.A. Wang, R. Ran, ACS Appl. Mater. Interfaces **8**, 8670 (2016)
45. M. Machida, M. Uto, D. Kurogi, T. Kijima, Chem. Mater. **12**, 3158 (2000)
46. D. Jiang, M. Zhang, G. Li, H. Jiang, Catal. Commun. **17**, 59 (2012)
47. G. Allaedini, S.M. Tasirin, P. Aminayi, Chem. Pap. **70**, 231 (2016)
48. Y. Wang, X. Li, L. Zhan, C. Li, W. Qiao, L. Ling, Ind. Eng. Chem. Res. **54**, 2274 (2015)
49. B. Bai, J. Li, J. Hao, Appl. Catal. B Environ. **164**, 241 (2015)
50. F. Chen, T. Yang, S. Zhao, T. Jiang, L. Yu, H. Xiong, C. Guo, Y. Rao, Y. Liu, L. Liu, J. Zhou, P. Tu, J. Ni, Q. Zhang, X. Li, Chin. Chem. Lett. **30**, 2282 (2019)
51. Y. Wang, C. Ge, L. Zhan, C. Li, W. Qiao, L. Ling, Ind. Eng. Chem. Res. **51**, 116677 (2012)
52. F. Xia, Z. Song, X. Liu, Y. Yang, Q. Zhang, J. Peng, Res. Chem. Intermed. **44**, 2703 (2018)
53. C. Sui, L. Xing, X. Cai, Y. Wang, Q. Zhou, M. Li, Catalysts **10**, 243 (2020)
54. Y. Wang, W. Deng, Y. Wang, L. Guo, T. Ishihara, Mol. Catal. **459**, 61 (2018)
55. G. Picasso, M. Gutierrez, M.P. Pina, J. Herguido, Chem. Eng. J. **126**, 119 (2007)
56. L. Li, Y. Diao, X. Liu, J. Rare Earths **32**, 409 (2014)
57. A. Chen, H. Guo, Y. Song, P. Chen, H. Lou, Int. J. Hydrogen Energy **42**, 9577 (2017)
58. S.D. Gupt, R.L. Stewart, D. Chen, K.A. Abboud, H. Cheng, S. Hill, G. Christou, Inorg. Chem. **59**, 8716 (2020)
59. G. Liu, R. Yue, Y. Jia, Y. Ni, J. Yang, H. Liu, Z. Wang, X. Wu, Y. Chen, Particuology **11**, 454 (2013)
60. P. Raghavendrachar, S. Ramachandran, Ind. Eng. Chem. Res. **31**, 453 (1992)
61. W. Partenheimer, J. Mol. Catal. A Chem. **206**, 105 (2003)

Authors and Affiliations

Gui Chen[1,3] · Kuiyi You[1,2] · Fangfang Zhao[1] · Zhenpan Chen[1] · Hean Luo[1,2]

✉ Kuiyi You
kuiyiyou@xtu.edu.cn

✉ Hean Luo
hluo@xtu.edu.cn

[1] School of Chemical Engineering, Xiangtan University, Xiangtan 411105, People's Republic of China

[2] National & Local United Engineering Research Center for Chemical Process Simulation and Intensification, Xiangtan University, Xiangtan 411105, People's Republic of China

[3] College of Chemistry and Materials, Huaihua University, Huaihua 418000, People's Republic of China